NACA

RESEARCH MEMORANDUM

A PRELIMINARY INVESTIGATION AT MACH NUMBER 1.91 OF AN INLET CONFIGURATION DESIGNED FOR INSENSITIVITY TO POSITIVE ANGLE-OF-ATTACK OPERATION

By Milton A. Beheim

Lewis Flight Propulsion Laboratory
Cleveland, Ohio

NATIONAL ADVISORY COMMITTEE
FOR AERONAUTICS

WASHINGTON
July 10, 1953

NATIONAL ADVISORY COMMITTEE FOR AERONAUTICS

RESEARCH MEMORANDUM

A PRELIMINARY INVESTIGATION AT MACH NUMBER 1.91 OF AN INLET CONFIGURATION DESIGNED FOR INSENSITIVITY TO POSITIVE ANGLE-OF-ATTACK OPERATION

By Milton A. Beheim

SUMMARY

A preliminary investigation was conducted to determine the pressure-recovery and mass-flow characteristics of an inlet configuration designed to be less sensitive to positive angle-of-attack operation than is a conventional conical inlet. The inlet consisted of half of an axially symmetric supersonic diffuser with conical centerbody. Flat plates with both straight and swept leading edges were used as the upper surface. The investigation was conducted at a Mach number of 1.91 over an angle-of-attack range from -5° to 14°.

Decreased sensitivity to positive angles of attack but increased sensitivity to negative angles was demonstrated. Up to angles of attack from 8° to 12°, depending upon the upper-surface plate configuration, the peak pressure recoveries were greater than at 0°; while at a 14° angle of attack the peak recoveries were 3 to 7 percent less than at 0°. Critical mass-flow ratios were greater than at zero angle of attack throughout the positive angle-of-attack range to at least 13°.

INTRODUCTION

Experimental investigations of the angle-of-attack performance of conventional conical-centerbody supersonic diffusers demonstrate reductions in critical mass flow and peak pressure recovery with increasing angles of attack (e.g., refs. 1 and 2). The decreased supercritical mass flow resulted from a decreased projected inlet area, from spillage around the cowl in regions where the shock wave from the cone moved increasingly upstream of the cowl lip, and from shock detachment at the cowl lip. The decreased pressure recovery may have resulted from several causes, including (1) upwash around the cone with a thickened boundary layer and sometimes separation on the lee side, (2) large flow angularities and Mach number gradients in the region of the throat, with mixing

losses as well as the attendant difficulties in stabilizing the terminal shock wave in the minimum area, (3) nonoptimum compression from the initial shock wave generated by the cone at angle of attack.

Although decreased pressure recovery generally means decreased engine thrust, very moderate increases in angle of attack may result in large aircraft drag increases that can dwarf the changes in thrust resulting from the inlet performance. However, because complete criteria by which to determine a satisfactory inlet for operation at high angles of attack have not as yet been established, an investigation is being conducted of inlet configurations designed to maintain high pressure recovery and high mass-flow ratios at angle of attack.

In reference 3 an investigation was conducted of an inlet employing a vertically oriented wedge compression surface designed to alleviate the unfavorable phenomena associated with angle of attack. This study of inlet types is continued in the present investigation, which was conducted at a Mach number of 1.91 over an angle-of-attack range from -5° to 14°. Half of a conventional conical-centerbody supersonic diffuser was used as the basic configuration. A flat splitter plate that comprised the upper surface of the diffuser prevented flow spillage due to upwash around the half cone. At positive angles of attack this plate also served as an additional compression surface, reduced upwash on the cone surface, and reduced the Mach number gradient at the annular throat, all relative to the conventional conical diffuser. Various geometries of the upper plate were included in the study. The investigation was conducted at the NACA Lewis laboratory.

SYMBOLS

The following symbols are used in this report:

A	area
m	mass flow
P	total pressure
R	inlet radius
T	total temperature
W_a	weight of air flow, lb/sec
x	lineal distance
α	angle of attack

δ ratio of total pressure following diffusion to NACA sea-level standard pressure, $P_1/29.92$

θ ratio of total temperature to NACA sea-level standard temperature, $T/519$

Subscripts:

c critical

i inlet

m maximum

t throat

0 free-stream condition

1 condition at exit of subsonic diffuser

APPARATUS

The investigation was conducted in the 18- by 18-inch wind tunnel at a Mach number of 1.91 and a Reynolds number of 3.9×10^5 based on cowl-lip diameter. The stagnation-air temperature was 150° F, and the inlet dew point varied from 0° to -36° F.

The model inlet utilized in the investigation was the same as that in the side-inlet investigation of reference 4, except that the extended flat plate used to generate an initial boundary layer and the boundary-layer removal system were eliminated. The resulting nose inlet (fig. 1(a)) had a 25°-half-angle cone, with the cowl lip positioned so that at the test Mach number the theoretical maximum mass-flow ratio was 0.95 (ref. 5). No internal contraction was provided in the inlet, as indicated in figure 1(b).

A variety of splitter-plate geometries was obtained by varying the sweep of the plate leading edge. The location of the plate in relation to the inlet is shown in figure 2(a). Figure 2(b) is a sketch of a plate having no sweep, while figure 2(c) shows a plate with the leading edge swept $47\frac{1}{2}°$ from the tip of the cone to the lip of the cowl. Plates with leading edges swept 42° and 24° are shown in figures 2(d) and 2(e), respectively. The angle of the plate in the vertical plane at the leading edge was sufficiently small to preclude shock detachment at zero° angle of attack in all cases. The boundary layer on the plate swept $47\frac{1}{2}$

was modified with a 1/8-inch-wide strip of number 100 carborundum dust located 1/8 inch downstream of the leading edge of the plate. Additional modification to the $47\frac{1}{2}^{\circ}$-swept plate included the use of perforations and of a slot downstream of the throat as indicated in figures 2(f) and 2(g).

Total-pressure-recovery measurements were made with a rake of 13 pitot-static tubes located 7 inches downstream of the end of the subsonic diffuser (fig. 3); pressures were recorded on a tetrabromoethane multimanometer system. Mass-flow measurements were obtained with a standard A.S.M.E. orifice. Angle of attack was varied with the support strut and determined by reading the heights of two reference points on the model with a cathetometer. At each angle of attack the exit pressure and mass flow were varied by the positioning of a butterfly valve, also shown in figure 3.

RESULTS AND DISCUSSION

The performance of each configuration investigated will be presented first in terms of its pressure recovery with mass-flow variations throughout the angle-of-attack range before a comparison is made of the various configurations. All inlet configurations differ only by the various splitter-plate geometries and, hence, will be identified by reference to the particular plate used. Some of the effects on inlet performance of detailed variations in the splitter-plate geometry may be peculiar to the low Reynolds number range of the subject investigation.

Straight Plate

The variation of total-pressure recovery with mass-flow ratio for the configuration with the straight-leading-edge plate is shown in figure 4(a). The supercritical mass-flow ratio at zero angle of attack was greater than the theoretical value; the measuring technique was checked by operating this inlet as a normal-shock inlet and was accurate to within 1/2 percent. Schlieren photographs of the shock-wave geometry also indicated a higher mass-flow ratio than the theoretical. This difference may have been caused by bluntness of the half-cone tip resulting from wear. As the angle of attack increased in the positive direction up to $5\frac{1}{2}^{\circ}$, the peak pressure recovery and critical mass-flow ratio also increased. Beyond $5\frac{1}{2}^{\circ}$ both quantities decreased, and at negative angles of attack decreased rapidly. The range of stable subcritical operation was improved up to positive angles of attack of approximately 13° and maximized near 6°. At negative angles of attack this stability range diminished and at -5° had vanished.

The shock patterns of this inlet at four angles of attack are shown in figure 5(a). The inner oblique wave was a disturbance originating from the plate leading edge. Beyond angles of attack of about 10°, a bow shock from the lip existed in front of the inlet throughout the stable range of operation.

Plate Swept $47\frac{1}{2}^\circ$

The variations of total-pressure recovery with mass-flow ratio for the inlet with the plate swept $47\frac{1}{2}^\circ$ are presented in figure 4(b). The rate of change with angle of attack of both peak pressure recovery and critical mass flow of the inlet using this plate was less than that of the straight-plate inlet, but followed the same trends. The range of stable subcritical operation at zero angle of attack and throughout the positive angle-of-attack range was also much less. An unexpected result was that, at zero angle of attack, the peak pressure recovery with the plate swept $47\frac{1}{2}^\circ$ was $2\frac{1}{2}$ percentage points less than that with the straight plate. Roughness was added to the leading edge of the swept plate in an attempt to approximate the thicker and possibly turbulent boundary layer on the straight plate downstream of the conical shock wave. The effect, however, was a decrease in pressure recovery of 3 percentage points at zero angle of attack, with diminishing effect as the positive angle of attack increased.

As seen in figure 5(b), the shock patterns were similar to those with the straight plate at critical mass flow, except that the disturbance from the plate leading edge was no longer evident. Furthermore, at the high positive angles of attack, the strength of the oblique shock was not as great. Because of the very low range of stable subcritical operation with this swept plate, the shock patterns were substantially the same at peak pressure recovery as at critical mass flow and, hence, are not presented.

Plates Swept 42° and 24°

Because the cowl lip was positioned for supersonic spillage, the leading edge of the plate swept $47\frac{1}{2}^\circ$ fell slightly behind the 44° conical shock. To establish quantitatively the effect of the sweep of the plate leading edge on the inlet pressure recovery, the angle of sweep was first decreased to 42° so that the leading edge was slightly upstream of the oblique shock. This configuration, however, gave a peak pressure recovery 2 percentage points less than that with the plate swept $47\frac{1}{2}^\circ$ at zero angle of attack. The plate swept 24° (which had approximately half as

much sweepback as the plate swept $47\frac{1}{2}^{\circ}$ and, therefore, an average plate length about midway between that of the straight plate and the plate swept $47\frac{1}{2}^{\circ}$) enabled a peak pressure recovery to be reached that was 1 percentage point higher than that with the plate swept $47\frac{1}{2}^{\circ}$. These detailed variations are not well understood.

Perforated Plates

Unpublished data on the motion of tufts located on the inner surfaces of the inlet show that separation of the boundary layer behind the normal shock exists on the cone surface and on the plate near the intersection of the plate and the cone. In an attempt to reduce this separation of the boundary layer, holes were drilled downstream of the throat in the plate swept $47\frac{1}{2}^{\circ}$. The use of three such rows of holes gave substantial improvements in the peak pressure recovery and in the range of stable subcritical operation. Each row of holes was then checked singly at zero angle of attack to determine an optimum location. Row 1, located just downstream of the throat, did not improve the peak pressure recovery. Row 2 gave an improvement of $1\frac{1}{2}$ percentage points in peak pressure recovery. The effect of row 3 was a decrease in peak pressure recovery of 4/5 percentage point compared with that achieved using the second row. However, the peak pressure recovery and range of stable subcritical operation of the inlet with the three rows of holes were higher than with row 2 alone. With the optimum location of row 2, an area for flow bleed approaching that for the three-row configuration was achieved with a 1/16-inch-wide slot in the plate extending across the inlet. The performance of this configuration is shown in figure 4(c). At zero angle of attack, the peak pressure recovery of this configuration was equal to that with the straight plate. In the angle-of-attack range from -5° to 9°, the stable subcritical range was substantially greater than that of the other configurations of this investigation.

The supercritical mass flow began to drop for the slotted plate at a total-pressure recovery less than that at critical operation with the solid plate. This drop occurred because the flow through the slot increased as the normal shock moved upstream and increased the pressure differential across the slot. This change in the flow is indicated in figure 5(c) by the appearance of a stronger external shock from the flow through the slot at peak pressure recovery than that during the highly supercritical operation. It is immediately obvious that the slot enabled the normal shock to move further upstream of the inlet at peak pressure recovery. Instability may finally have occurred as a result of the vortex sheet from the intersection of the oblique shock and the normal shock intersecting the cowl lip (ref. 6).

The progressive extension of the stable subcritical range of the inlet with the plate swept $47\frac{1}{2}^{\circ}$ with variations of the location and amount of flow bleed at zero angle of attack is shown in figure 4(d). At most there was only a 2-percent loss in supercritical mass flow through the holes or the slot.

General Comparison

The variation of peak pressure recovery and critical mass flow with angle of attack of the various configurations can be seen in figure 6. Peak pressure recoveries were greater than at zero angle of attack up to angles of attack of from 8° to 12°, depending upon the plate configuration. At 14° the peak recoveries were from 3 to 7 percent less than at 0°. The effectiveness of the slot in improving the pressure recovery of the swept-plate configuration in the angle-of-attack range below 10° is clearly evident. The peak pressure recovery of the inlet with this plate was superior to that with the straight plate over most of the angle-of-attack range investigated. This was particularly true at negative angles of attack, where the stronger expansion from the plate with the straight leading edge had a very detrimental effect on the inlet pressure recovery.

Critical mass-flow ratios exceeded the values at zero angle of attack up to angles of attack of at least 13°. The increase in external compression with increased positive angles of attack resulted in this increase in the critical mass flow, until the displacement of the external shock waves was such that the decrease in flow resulted. It is significant to note that the high values of mass-flow ratio at large angles of attack are not indicative of small amounts of spillage. In particular, the straight-plate configuration, which yielded mass flows comparable to those obtained with the swept plate of smaller projected area at angle of attack, would capture less of all the air compressed and would hence be subject to higher drag. Because of the expansion of the flow at negative angles of attack, the critical mass flow was reduced during such operation.

Also presented in figure 6 are the variations with angle of attack of the corrected weight flow of air per unit frontal area of the inlet, $W_a\sqrt{\theta}/\delta A_1$. A turbojet-engine operating line for constant Mach number, altitude, and engine rotational speed is represented by a constant value of the weight-flow parameter, the particular value being at the discretion of the designer. To illustrate the significance of the plot, consider the slotted-plate configuration: If the inlet and engine were matched at zero angle of attack so that the inlet operated at critical mass flow, the inlet would remain approximately so throughout the entire angle-of-attack range, provided that engine operation is subject

to the above restrictions. If the inlet were matched for operation at peak pressure recovery at zero angle of attack, the inlet mass-flow ratio would have to be decreased below that corresponding to peak recovery at angles of attack greater than 6° and at all negative angles. With this inlet, unstable operation would result. It is thus illustrated that inlet-engine matching at angle of attack can be an important consideration.

The variations with angle of attack of peak pressure recovery and critical mass flow relative to the values at zero angle of attack are presented in figure 7 for the half-cone inlet with the slotted plate swept $47\frac{1}{2}^\circ$, the vertical wedge inlet (asymmetrical cowl) of reference 3, and a conventional conical-centerbody inlet. Not shown by this figure is the fact that, at zero angle of attack, the peak pressure recovery of the half-cone inlet and the conical inlet was approximately the same but about 5 percent greater than that of this particular wedge inlet.

Contour maps indicated velocity profiles following diffusion at zero angle of attack similar to those reported in reference 4. This particular subsonic diffuser design was such that separation occurred on the centerbody side of the duct. At angle of attack, the profile remained essentially unchanged for the inlet with the straight-leading-edge splitter plate. With the plates swept $47\frac{1}{2}^\circ$, the region of highest Mach number shifted with angle of attack, until at 14° the indicated region of separated flow was relocated on the opposite side. The initially poor velocity profiles did not improve appreciably with angle of attack and, hence, are not presented. Uniformity of the velocity profiles at the compressor-inlet station may be an important inlet characteristic at angle of attack. Satisfactory criteria have not yet been generally established as to the permissible gradients; however, it is felt that any inlet, such as the present one, which reduces the circumferential Mach number gradient at the inlet throat would offer inherent advantages in this respect.

SUMMARY OF RESULTS

A preliminary investigation was conducted to determine mass-flow and pressure-recovery characteristics of an inlet designed for relative insensitivity in these respects to angle of attack. The supersonic diffuser consisted of half of a conventional conical-centerbody diffuser and a flat plate with both straight and swept leading edges as the upper surface. At a Mach number of 1.91 and in an angle-of-attack range from -5° to 14° the following results were obtained:

1. Peak pressure recoveries exceeded the values at zero angle of attack up to angles of attack from 8° to 12°, depending upon details of the upper-surface plate design; at 14° the peak recoveries obtainable were from 3 to 7 percent below the values at zero angle of attack.

2. Critical mass-flow ratios were greater than at 0° throughout the positive angle-of-attack range to at least 13°.

3. At negative angles of attack, both peak pressure recoveries and critical mass-flow ratios decreased.

Lewis Flight Propulsion Laboratory
National Advisory Committee for Aeronautics
Cleveland, Ohio, May 5, 1953

REFERENCES

1. Englert, Gerald W., and Obery, Leonard J.: Evaluation of Five Conical Center-Body Supersonic Diffusers at Several Angles of Attack. NACA RM E51L04, 1952.

2. Perchonok, Eugene, Wilcox, Fred, and Pennington, Donald: Effect of Angle of Attack and Exit Nozzle Design on the Performance of a 16-Inch Ram Jet at Mach Numbers from 1.5 to 2.0. NACA RM E51G26, 1951.

3. Leissler, L. Abbott, and Hearth, Donald P.: Preliminary Investigation of Effect of Angle of Attack on Pressure Recovery and Stability Characteristics for a Vertical-Wedge-Nose Inlet at Mach Number of 1.90. NACA RM E52E14, 1952.

4. Goelzer, H. Fred, and Cortright, Edgar M., Jr.: Investigation at Mach Number 1.88 of Half of a Conical-Spike Diffuser Mounted as a Side Inlet with Boundary-Layer Control. NACA RM E51G06, 1951.

5. Sibulkin, Merwin: Theoretical and Experimental Investigation of Additive Drag. NACA RM E51B13, 1951.

6. Ferri, Antonio, and Nucci, Louis M.: The Origin of Aerodynamic Instability of Supersonic Inlets at Subcritical Conditions. NACA RM L50K30, 1951.

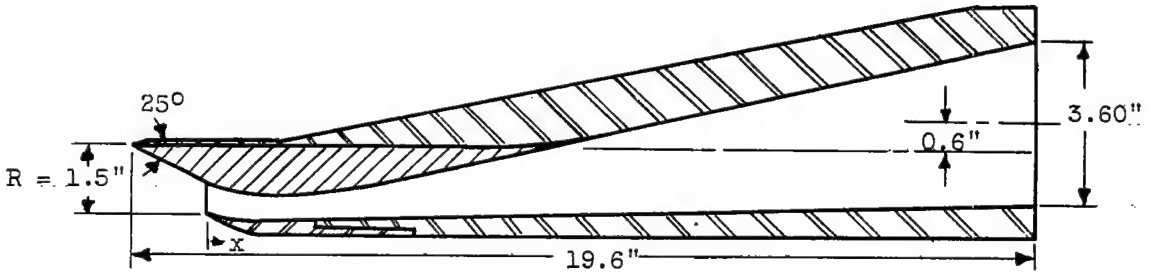

(a) Cross section of model.

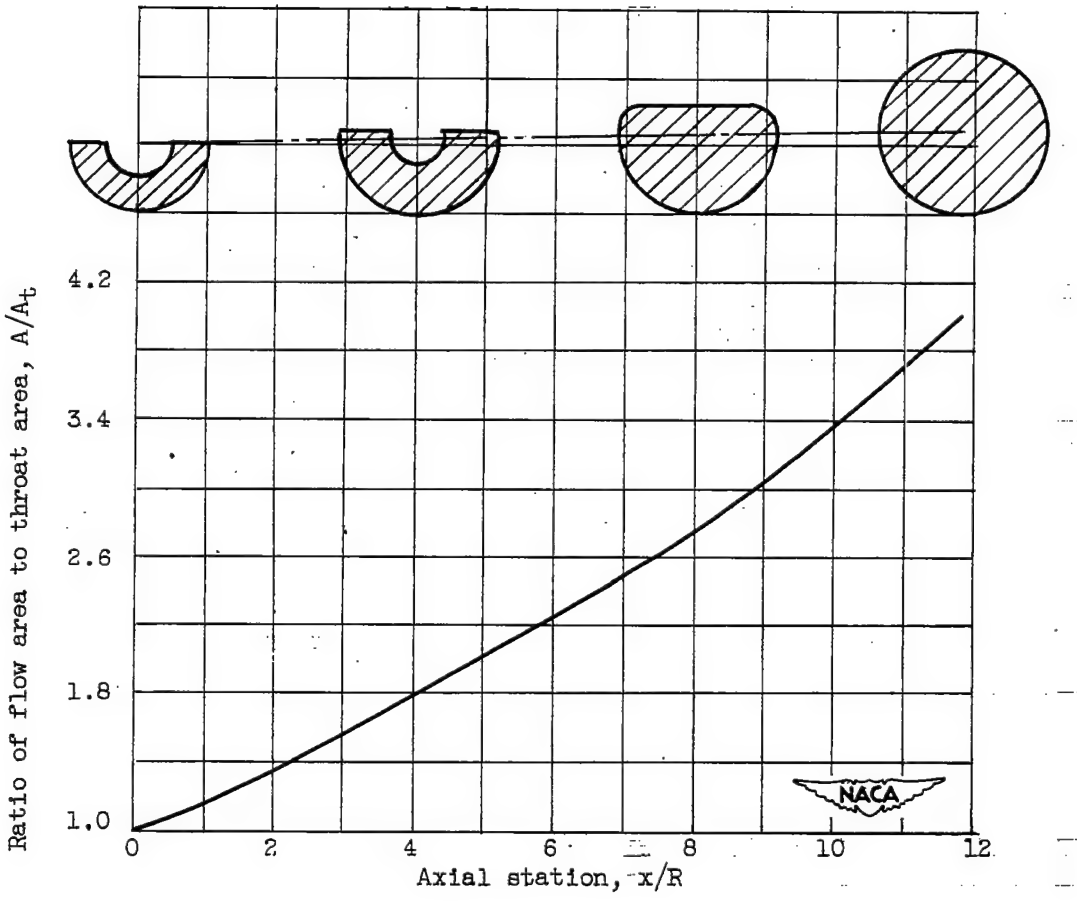

(b) Area variations.

Figure 1. - Dimensions and cross-sectional area variations of model inlet.

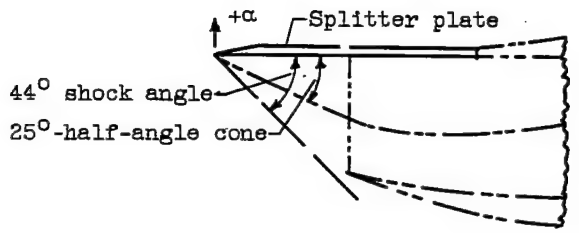

(a) Side view.

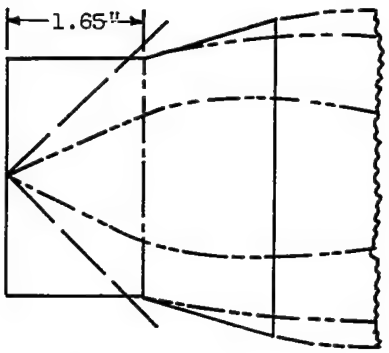

(b) Straight plate.

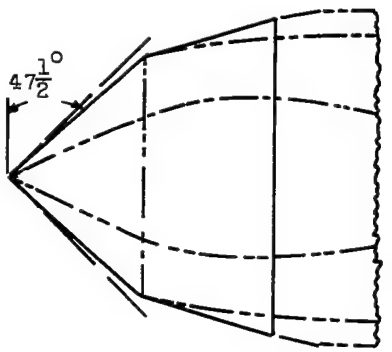

(c) Plate swept 47½°.

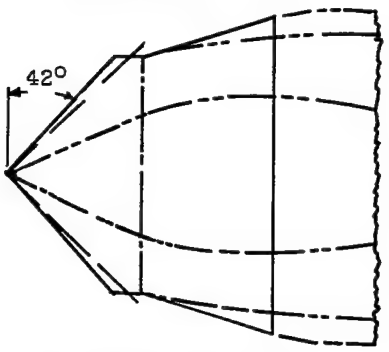

(d) Plate swept 42°.

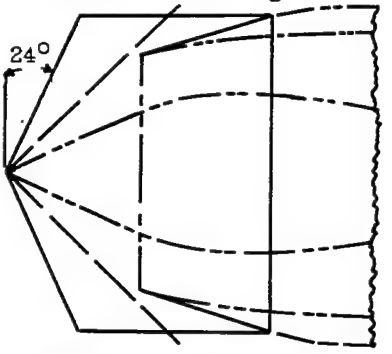

(e) Plate swept 24°.

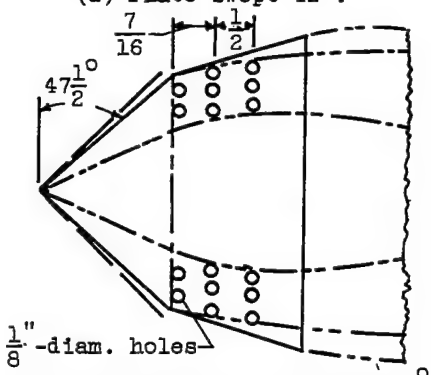

(f) Perforated plate swept 47½°.

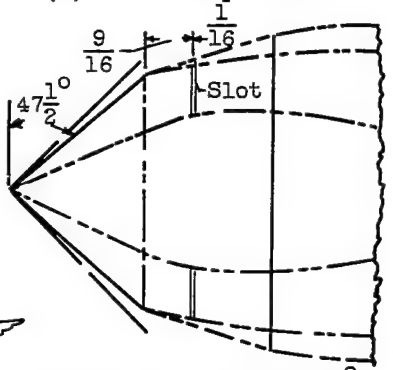

(g) Slotted plate swept 47½°.

Figure 2. - Splitter-plate dimensions and modifications.

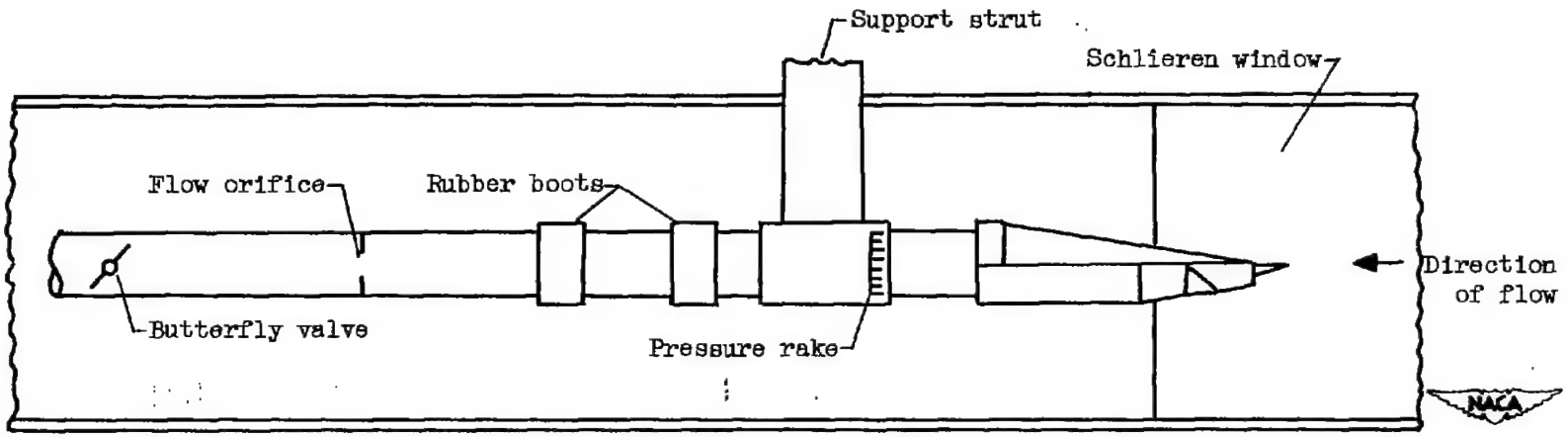

Figure 3. - Schematic diagram of model installation in 18- by 18-inch wind tunnel.

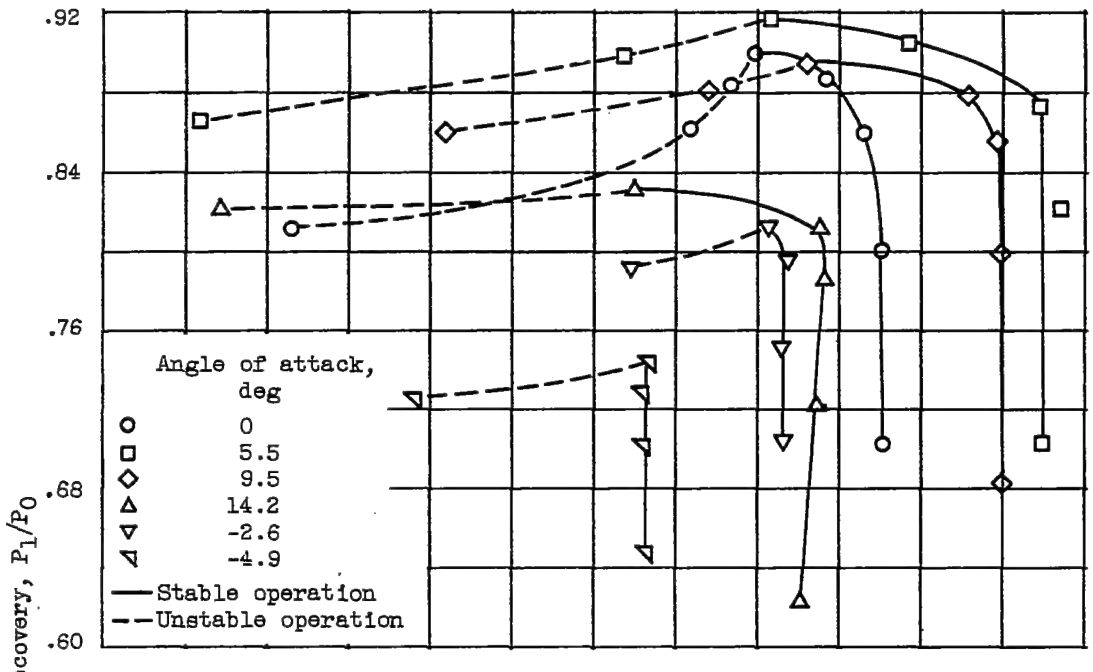

(a) Splitter plate with straight leading edge.

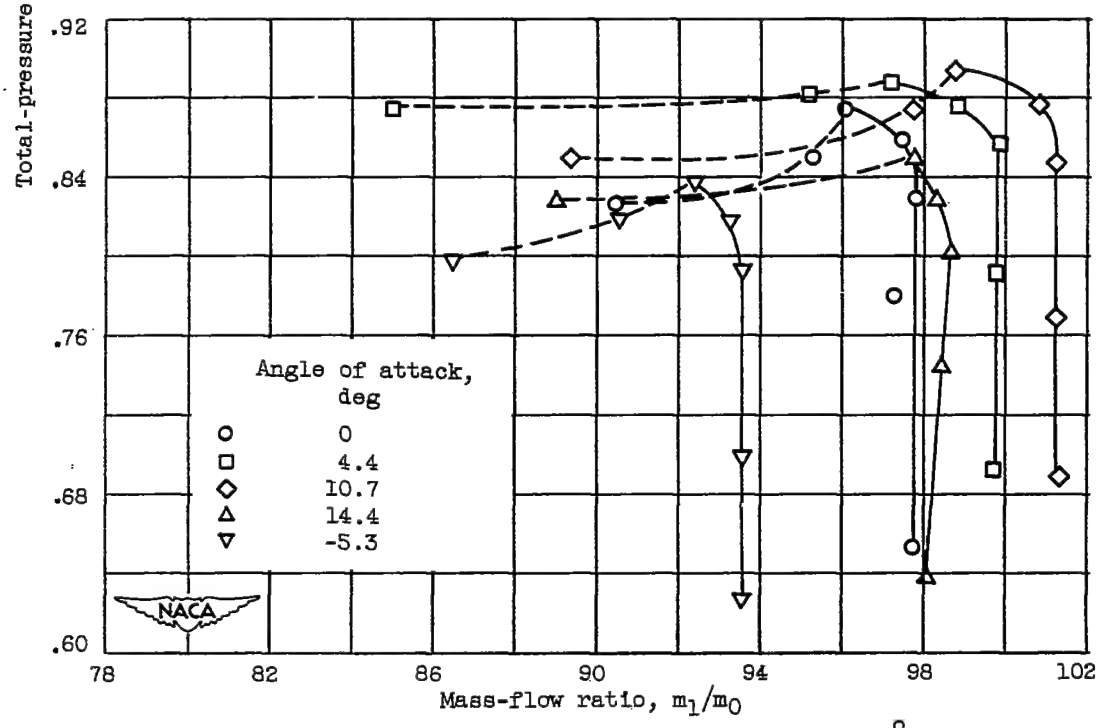

(b) Splitter plate with leading edge swept $47\frac{1}{2}^\circ$.

Figure 4. - Inlet total-pressure recovery as function of mass-flow ratio at various angles of attack with varied splitter plates.

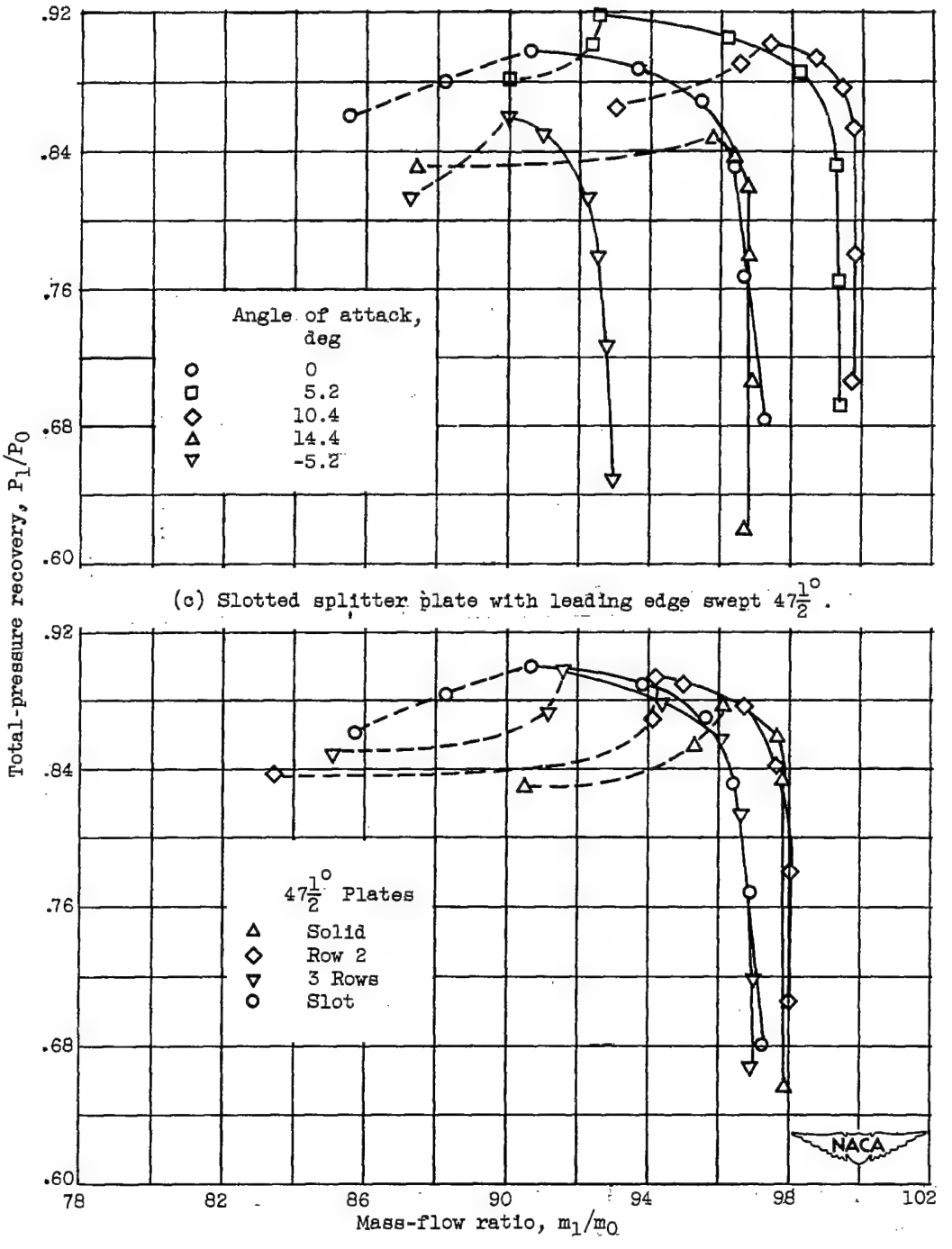

(c) Slotted splitter plate with leading edge swept $47\frac{1}{2}^\circ$.

(d) Modified splitter plates at zero angle of attack with leading edge swept $47\frac{1}{2}^\circ$.

Figure 4. - Concluded. Inlet total-pressure recovery as function of mass-flow ratio at various angles of attack with varied splitter plates.

Critical mass flow

Peak pressure recovery

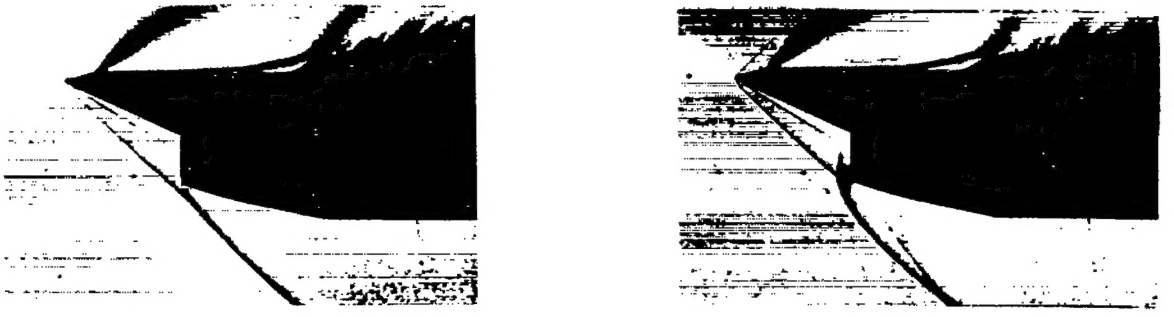

Angle of attack, 0°.

Angle of attack, 6°.

Angle of attack, 14°.

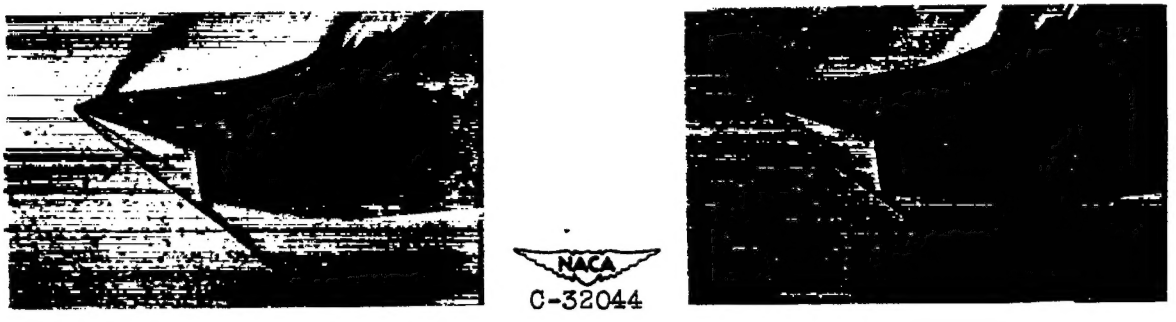

Angle of attack, -5°.

(a) Splitter plate with straight leading edge.

Figure 5. - Schlieren photographs of inlet at various angles of attack with varied splitter plates.

Angle of attack, 0°

Angle of attack, 14°

Angle of attack, -5°

(b) Splitter plate with leading edge swept $47\frac{1}{2}^\circ$. Critical mass flow.

Supercritical mass flow; angle of attack, 0°

Peak pressure recovery; angle of attack, 0°

NACA C-32807

(c) Slotted splitter plate with leading edge swept $47\frac{1}{2}^\circ$.

Figure 5. - Concluded. Schlieren photographs of inlet at various angles of attack with varied splitter plates.

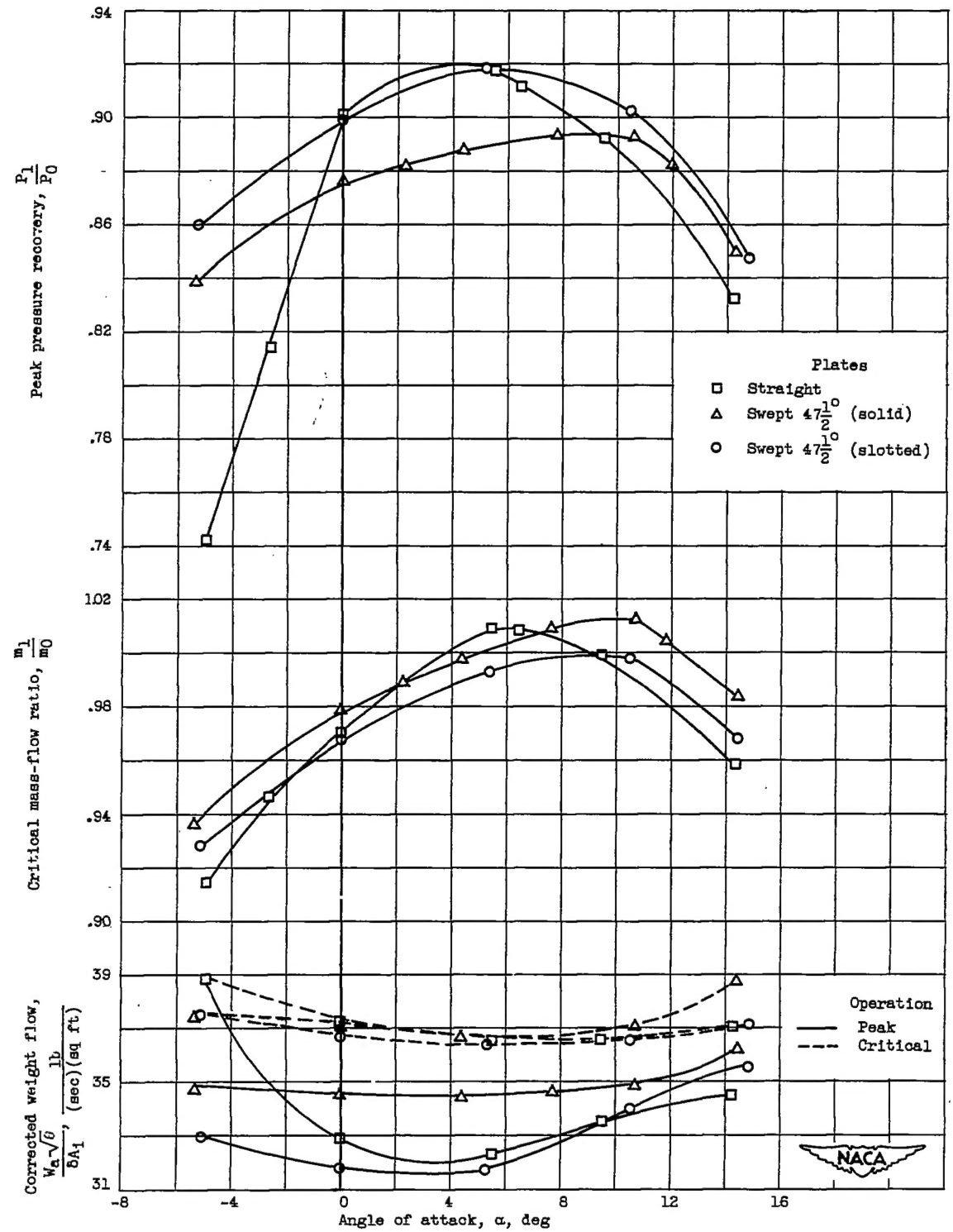

Figure 6. - Variations of peak pressure recovery, critical mass-flow ratio, and corrected weight flow with angle of attack of inlet utilizing various splitter plates.

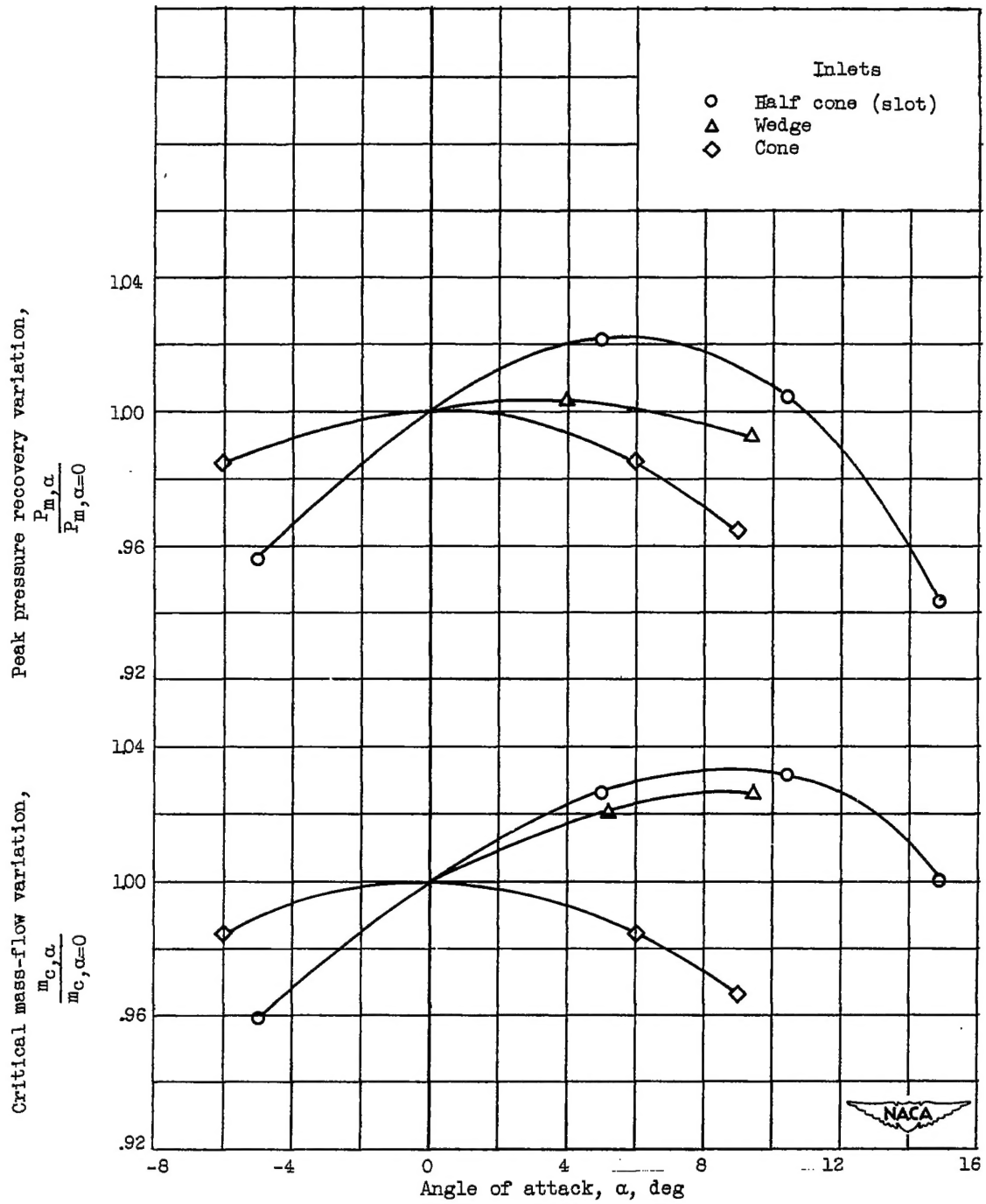

Figure 7. - Comparison at Mach number 1.9 of variations in peak pressure recovery and critical mass-flow ratio with angle of attack of various inlets.

NACA-Langley - 7-10-53 - 425